MARMARA UNIVERSITY
INSTITUTE FOR GRADUATE STUDIES
IN PURE AND APPLIED SCIENCES

ANTIMONY RECOVERY FROM VARIOUS ANTIMONY SOLUTIONS BY CEMENTATION AND PROCESS OPTIMIZATION

ABDULLAH UYSAL

(524717006)

MASTER THESIS

Department of Metallurgical and Materials Engineering

Thesis Supervisor

Doç. Dr. Serdar AKTAŞ

ISTANBUL, 2019 - YL

MARMARA UNIVERSITY
INSTITUTE FOR GRADUATE STUDIES IN PURE AND APPLIED SCIENCES

Abdullah UYSAL, a Master of Science student of Marmara University, Institute for Graduate Studies in Pure and Applied Sciences, defended his thesis entitled "Antimony recovery from various antimony solutions by cementation and process optimization", on 27.12.2019 and has been found to be satisfactory by the jury members.

Jury Members

Assoc.Prof.Dr. Serdar AKTAŞ (Advisor)
Marmara University .....

Prof.Dr. Cevat SARIOĞLU (Jury Member)
Marmara University .....

Assoc.Prof.Dr. Bihter ZEYTUNCU (Jury Member)
Istanbul Technical University .....

APPROVAL

Marmara University Institute for Graduate Studies in Pure and Applied Sciences Executive Committee approves that Abdullah UYSAL be granted the degree of Master of Science in Department of Metallurgical and Materials, Metallurgical and Materials Program on 02.01.2020 (Resolution no: 2020/01-02).

Director of the Institute
Prof. Dr. Bülent EKİCİ

ACKNOWLEDGEMENT

I wish to thank Dr. Serdar Aktaş and Research Assistant Burcu Nilgün Çetiner for helping me through the whole thesis process. I am so thankful for their encouragement and feedback. I appreciate Dr.Aktaş for sparking my interest in this subject and having his guidance during this research period. This project was funded by Marmara University Scientific Research Unit under the project FEN-C-YLP-170419-0122. So I wish to thank all committee members for their support and MC365 Laboratory staff for assisting me with patience through long experiments. It was a great experience to be able to work with all of them and hope this study will contibute some valuable information to the scientific literature.

Thank You All!

12/2019 **Abdullah UYSAL**

Table of Contents

ACKNOWLEDGEMENT i
ÖZET iv
SUMMARY v
SYMBOLS vi
ABBREVIATIONS vii
LIST OF FIGURES viii
LIST OF TABLES x
1. INTRODUCTION 11
2. BACKGROUND 13
2.1. Antimony 13
2.1.1. Uses and applications 13
2.1.2. Physial and Chemical Properties of Antimony 14
3. THEORY 17
3.1. Cementation of Antimony Using Metallic Zinc 17
4. MATERIALS & METHODS 21
4.1. Materials Used in the Experiments 21
4.2. Process Layout of Experiments 21
4.3. Dissolution of Antimony(III) Chloride 23
4.4. Determination of Antimony Concentration 23
4.4.1. Bromatometric Titration Method 25
4.5. Production and Characterization of Metallic Antimony 26
4.6. Determination of Zinc Concentration 28
5. RESULTS and DISCUSSION 29
5.1. Effects of Parameters on Cementation Efficiency 29
5.1.1. Effect of zinc quantity 29
5.1.2. Effect of temperature 30
5.1.3. Effect of reaction time 31
5.1.4. Effect of initial concentration 34
5.1.5. Effect of shaking speed 36
5.2. Optimization Studies to Increase Cementation Efficiency 37
5.3. Characterization of the Cementation Product 38
6. CONCLUSIONS 45
7. REFERENCES 47

ÖZET

ANTIMONY RECOVERY FROM VARIOUS ANTIMONY SOLUTIONS BY CEMENTATION AND PROCESS OPTIMIZATION

Birincil kaynaklardan antimon eldesi endüstride yaygın bir şekilde kullanılmaktadır. Bu kaynakların azalmasından dolayı ikincil kaynaklardan antimon geri dönüşümü gittikçe önemli hale gelmektedir. Günümüzde bazik çözeltilerden antimon geri dönüşümü ile ilgili birçok araştırma mevcuttur fakat antimonun asidik ortamdaki davranışı çok iyi bilinmemektedir. Antimon içeren endüstriyel atık çözeltilerin miktarı dikkate alındığında bu çalışmada elde edilecek verinin literatürdeki bir boşluğu dolduracağı, ekonomik ve endüstriyel açıdan fayda sağlayacağı açıktır.

Mevcut çalışmanın amacı metalik çinko yardımıyla sementasyon yöntemi ile antimon içeren asidik çözeltilerden antimon geri kazanımıdır. Sıcaklık, çinko miktarı, karıştırma oranı ve pH parametrelerinin sementasyon verimi üzerindeki etkileri detaylı bir şekilde incelenmiştir. Optimum reaksiyon verimi 25°C 3M HCl ve stokiyometrik-5 oranında Zn/Sb(III) kullanılarak 5 dakika reaksiyon süresi sonunda elde edilmiştir. Stok çözeltide bulunan antimonun 99.2% si sementasyon prosesi sonucunda geri kazanılmıştır. pH ölçümleri kullanılan fazla çinko metalinin ortamdaki serbest asit tarafından tüketildiğini göstermiştir. Beklenenin aksine reaksiyon süresi ve sıcaklık parametrelerinin antimon geri kazanımı üzerindeki etkisi olumsuzdur.

XRD difraksiyon analizi sonucunda sementasyon yöntemi ile elde edilen toz ürünün tüm difraksiyon piklerinin antimon metalik fazına ait olduğunu gözlenmiştir. Toz tane yapısının homojen ve yüksek saflıkta olduğu SEM analizi ile kanıtlanmıştır.

Bu çalışmada uygulanan proses kolay uygulanabilir, güvenilir ve ekonomik olduğundan dolayı elde edilen sonuçlar antimonun asidik atık çözeltilerden geri kazanımı ve sementasyon davranışı konusunda endüstri için bir kaynak teşkil edebilir.

SUMMARY

ANTIMONY RECOVERY FROM VARIOUS ANTIMONY SOLUTIONS BY CEMENTATION AND PROCESS OPTIMIZATION

Antimony extraction from primary sources is widely used in industry. Due to its depletion, its recovery from secondary sources is becoming important. Nowadays there are many investigations based on the recovery of antimony from basic solutions but its behavior in the acidic medium is not very well known. Considering the amount of acidic industrial waste containing antimony, this novel data will fulfill a gap in the literature and will be beneficial for both economically and environmentally.

The aim of the present work is recovery of antimony from antimony-containing solutions. In this study, cementation method with metallic zinc powder was performed. The effect of parameters such as temperature, amount of zinc, stirring rate and pH on the yield of cementation were overall studied. The optimal qualifications were achieved at 25°C for 5 minute with Zn/Sb(III) stoichiometric ratio of 5 in the solution of 3M HCl. Almost most of the antimony ions were cemented out of the solution. The output of the cementation is more than 99.2%. pH measurements showed that excess zinc is preferentially consumed by free acid. Contrary to expectations, time and temperature have negative impact on the recovery (%) of the antimony.

The XRD diffraction pattern of the resulting powder obtained through cementation showed that all diffraction peaks belong to antimony metallic phase. SEM images proved that the structure of the high purity product was in regular shape.

Regarding the cementation behavior of antimony and its recovery from acidic waste solutions, the proposed process and the results presented in this study can be a guide for industry since it is feasible, straight forward and economical.

SYMBOLS

C_0 : Initial antimony concentration (%)

C_t : Final antimony concentration (%)

E° : Standard potential (V)

F : Faraday constant

G° : Standard free energy (j)

K_{eq} : Equilibrium constant

R : Constant

T : Temperature (°C)

ΔV : Increment of volume

Y : EDTA

In : Indicator

ABBREVIATIONS

AMU : Atomic Mass Unit

EDS : Energy Dispersive Spectroscopy

EDTA : Ethylene Diamine Tetraacetic Acid

EDX : Energy Dispersive X-ray Detector

RPM : Rotation per Minute

SEM : Scanning electron microscope

SHE : Standard Hydrogen Electrode

XRD : X-ray diffractometer

WHO : World Health Organization

LIST OF FIGURES

Figure 2:1: The stability interval of the generated compounds and lg[Sb^{3+}]-pH curves of antimony. 16
Figure 3:1: The schematic ilustration of a single zinc powder particle in the course of cementation process 17
Figure 4:1: Flow sheet of the applied process 22
Figure 4:2: Titration of the stock solution through automatic titrator before cementation process. 24
Figure 4:3: pH measurement after solid/liquid separation 25
Figure 4:4: Water bath unit with temperature and shaking control system 27
Figure 4:5: Zinc added solution samples on the modified shaking system of the water bath unit 27
Figure 4:6: Determination of the zinc content after cementation 28
Figure 4:7: Metallic antimony powder dried in the drying oven 28
Figure 5:1: Relation between antimony recovery and increasing amount of zinc at different temperatures. (25mL, 1000ppm Sb3+, 10g/L Tartaric acid, 60 rpm, 5 minutes) 30
Figure 5:2: Relation between antimony recovery and reaction time at different temperatures. (25mL, 1000ppm Sb3+, 10g/L Tartaric acid, shake, Stoichiometric ratio x1) 31
Figure 5:3: Relation between antimony recovery and reaction time at different temperatures. (25mL, 1000ppm Sb3+, 10g/L Tartaric acid, 60 rpm, Stoichiometric Ratio x3) 32
Figure 5:4: Comparison of the alteration in antimony recovery(%) with various amounts of zinc at constant temperature. (25mL, 1000ppm Sb3+, 10g/L Tartaric acid, 60 rpm, 25°C) 33
Figure 5:5: The change in antimony recovery(%) with various amounts of zinc at constant temperature. (25mL, 0.2M Sb3+, 3M HCl, 60 rpm, 25°C) 34
Figure 5:6: The ratio of dissolved zinc to the total amount of zinc added. (10g/L Tartaric acid, 60 rpm, 25°C, Stoichiometric x1) 35

Figure 5:7: The degrees of dissolved zinc (mg) with different amounts of zinc added to the solution (25mL, 1000ppm Sb3+, 10g/L Tartaric acid, 60 rpm, 120 minute, 25C)... 35
Figure 5:8: The degrees of dissolved zinc(mg) only used for cementation with different amounts of zinc added to the solution (25mL, 1000ppm Sb3+, 10g/L Tartaric acid, 60 rpm, 120 minute, 25C) 36
Figure 5:9: Precipitated form of zinc hydroxide after cementation 36
Figure 5:10: The effect of shaking and stirring on the cementation of antimony at constant temperature. (25mL, 1000ppm Sb3+, 10g/L Tartaric acid, 60 rpm, 25°C, Stoichiometric x1)..... 37
Figure 5:11: Comparison of one step and two step cementation in the basis of Sb recovery (25mL, 1000 ppm Sb3+, 3M HCl and 10g / L tartaric acid, 60 rpm, 5 minutes)..... 38
Figure 5:12: The result of XRF analysis in general metals mode with acquisition time of 61s..... 39
Figure 5:13: The XRD diffraction pattern of antimony powder cemented through stoichiometrically 5 times zinc addition. 40
Figure 5:14: SEM image of the antimony powder obtained through cementation by zinc powder. (25mL, 3M HCl, 60 rpm, 25°C, 5 minute) 40
Figure 5:15: SEM image of the metallic antimony powder gained through cementation by zinc powder. (25mL, 2M HCl, 60 rpm, 25°C, 5 minute) 41
Figure 5:16: SEM-EDS diagram of the antimony powder gained through cementation by zinc powder. (2M HCl, 60 rpm, 25°C, 5 minute) 42

LIST OF TABLES

Table 3.1: Selected standard reduction potentials in aqueous solutions at 25 °C vs. SHE [64]. 18
Table 4.1: Optimum settings for Sb^{3+} titration in automatic titrator..... 24

1. INTRODUCTION

High-grade ores have been extensively depleted due to the developing industry and increasing use of chemicals. Therefore, the importance of hydrometallurgical methods for recovering metallic values from industrial wastes as well as low tenor ores is increasing. [1-2]. Industrial waste solutions contain valuable metal ions and / or toxic components after chemical and hydrometallurgical processes. When these components exceed the critical level in industrial wastewater, it will cause environmental pollution. Therefore, the recovery of precious metals is important from both environmental and economical perspectives. [2-6].

Since antimony is considered as impurity in many industrial processes, some methods like solvent extraction [7], adsorption [8-10], sedimentation [11], reverse osmosis [12], biosorption [13-14], anion exchange [15], electrocoagulation [16], coagulation [17], and electrodeposition [18] were tested to remove antimony from aqueous solutions. Although the recovery rates are partially successful, there are some difficulties such as time consuming processes, high operating costs, adsorbents cause to secondary pollution and required recycling. [19].

Another significant hydrometallurgical process practiced for the recovery of ions in the metallic phase from leach or waste solutions in the industry, also for the treatment of the waste water is the cementation technique. It has been used in hydrometallurgy especially for the treatment of waste water for a long time. The recovery of precious metals in essentially pure metallic form has some advantages, such as low energy consumption and ease of control. [3, 20, 21]. The main disadvantages of the technique are the improper redox potential of sacrificing metal and excessive consumption of it [3,5,6]. The most common reducing agents in commercial applications are iron, zinc and aluminum. Among them zinc is generally preferred to recover noble metals such as rhodium [22], gold [23] and silver [24].

Cementation reactions may be identified on the redox reaction of a metal ion from an ionic solution to the metallic phase by a sacrificial metal. [3, 6, 25-26]. A cementation reaction can be described as

$$nA^{a+} + mB^{0} \rightarrow nA^{0} + mB^{b+} \quad (1.1)$$

where A, B represent the noble and the reducing metals respectively. Their stoichiometric coefficients and values are symbolized as n, m, a+ and b+ respectively. [3, 27].

Cementation of antimony has been studied by several researchers and is currently being investigated extensively. Zinc and aluminum are generally used as reducing metals in these researches [2, 4-6,8, 28-35].

Antimony pollution in wastewater systems caused by mining and smelting activities is an ecological and environmental problem. Although more research has been carried out in recent years, there are still gaps in the literature about cementation behavior of antimony from the waste solutions. The aim of this study is to investigate (1) pH-dependent release characteristics of Sb ions by cementation technique from Sb-bearing acidic solutions, (2) to investigate behavior of zinc as a cementator, and (3) to optimize the cementation conditions at a laboratory scale.

2. BACKGROUND

2.1. Antimony

2.1.1. Uses and applications

Antimony has been a known element since ancient times but its use was relatively limited. Demand for antimony has increased rapidly, especially in recent years with thriving automotive industry. It is the ninth most widely extracted element worldwide. It is generally imposed in ammunition alloys, as a catalyst in plastic synthesis or as flame retardant in industrial products. The rate of presence in natural underground resources is low. (Less than 1 mg / kg). [36]

Antimony alloys appear in many applications. Its alloys with lead used in bushing bearings offer low friction. Due to its anti-corrosion properties, it is used in soldering, pipes and roof plates. It is also applied as an electrode material in acid batteries, and the greatest metallic antimony recovery is provided by these accumulators. [37]

The most important antimony compound is antimony trioxide. Commercially available antimony trioxide is classified by particle size and contains less than 1% impurities such as arsenic, lead and iron. It is utilized as flame retardant component in textile, paint and plastic materials. Flame retardant applications include many components of plastics and textile materials in aerospace and automotive industry. It is also engaged in the composite industry with glass fibers as additives to polyester resins. The amount of antimony expended for fire prevention is about half of the annual antimony production [38]. It serves as a thinning agent by assisting in the removal of microscopic bubbles in optical glass production. This application is mainly used on TV screens [39].

Its increasing utilization as an alloying component such as gallium antimonite, aluminum antimonite and indium antimonite in semiconductor materials is remarkable [40]. Infrared detectors have begun to be exerted as a dopant for the production of diodes and for ultra high conductivity n-type silicon layers [41].

It is also widely employed as a pigment in paints. White colour is obtained by antimony oxides. Black and yellow colour pigments are obtained through antimony trisulfide and pentasulfide, respectively. Infrared radiation is preferred in antimony trisulfide

camouflage dyes due to their reflection properties. Antimony pentasulfide is used in red rubber production due to its vulcanizing properties.

Antimony compounds are frequently used in pesticides, drugs, catalysts and ammunition. It is one of the best lead alloy materials that can penetrate the armor plate, therefore extensively profited in the WW1.[38]

Compounds such as antimony potassium tartrate or tartar emetic, antiomalin or lithium antimony thiomat, meglumine antimoniate are used in biological or medical applications. Antimony is used in veterinary applications as it has a softening effect on keratinized tissues.

The flame retardants take the lead in the consumption of antimony with the percentage of 72%. Batteries and chemicals has the second highest consumption of antimony with 10% each which is followed by ceramics and glass with 4% each. The USA, European countries and Japan constitute 70% of the demand in general. [42]

2.1.2. Physial and Chemical Properties of Antimony

Antimony is found in column 15 of the periodic table. Sb is an element with atomic number 51 and an average mass of 121.76 amu with two isotopes. Its density is 6.69 g/cm^3. The oxidation state is similar to the arsenic which is just above in the periodic table.

Metallic antimony is a gray, bright, brittle semi-metal and found in nature as a natural mineral. [43-44]. It forms a rhombohedral crystal structure but under certain conditions it can form amorphous structures. This amorphous structure is less stable than the crystal structure. [45].

Antimony (III) can form complexes of halide, tartrate, sulfite and oxalate complexes in suitable medium. [46] But the linkage mechanism of the antimony to the organic substance has not been fully elucidated. Because the complex ligand structure of the organic compounds makes it difficult to define the chemical binding sites [47]. In some studies in the literature, antimony has been found to form stable complexes with chelating agents such as EDTA [48], citrate [49] or tartrate [50].

When pH < 3, the potential energy required for Sb^{3+} reduction is more negative than is required for hydrogen formation. In this case, Sb^{3+} ions are stable. However, when pH> 3, the Sb3+ reduction potential should be moved to a less negative potential to ensure solubility. This can be achieved by coordinating ligands. [51-57]. Gluconic, oxalic and tartaric acids are the most effective coordination ligands known in literature. The solubility of antimony and zinc in gluconic acid was examined by Eliaz et al [58]. It was observed that solution pH is an important parameter to consider in coordination chemistry. The application of Sb(III)-tartrate as standard can be recommended because of the better practicability (higher solubility and better redox stability compared to oxalic and gluconic acids) to prepare the Sb(III)-standard solution before cementation with zinc. [59]

Antimony (III) ions can be hydrolyzed and precipitated in the solutions containing chlorine. The concentration of Cl and OH- determines the stability of the $SbCl_3$ system. When this equilibrium changes, the antimony ion may form precipitate or the precipitate formed may dissolve again. Depending on the conditions, oxychloride compounds such as $Sb_4O_5C1_2$, Sb_2O_3, SbOCl may be formed according to this hydrolysis process. [60-61]. $SbCl_3$ undergoes hydrolysis in water or in moist environment to form antimony oxychloride: [62]

$$SbCl_3 + H_2O \leftrightarrow SbOCl + 2HCl \quad (2.8)$$

In the second step, SbOCl is converted to $Sb_4O_5C1_2$. The resulting oxide compounds are soluble in acidic media such as tartaric acid and hydrochloric acid. [59] In Figure 2.1, theoretically predicted the hydrolysis products depending on the pH of the Sb^{3+}-Cl-H_2O system [63] are given.

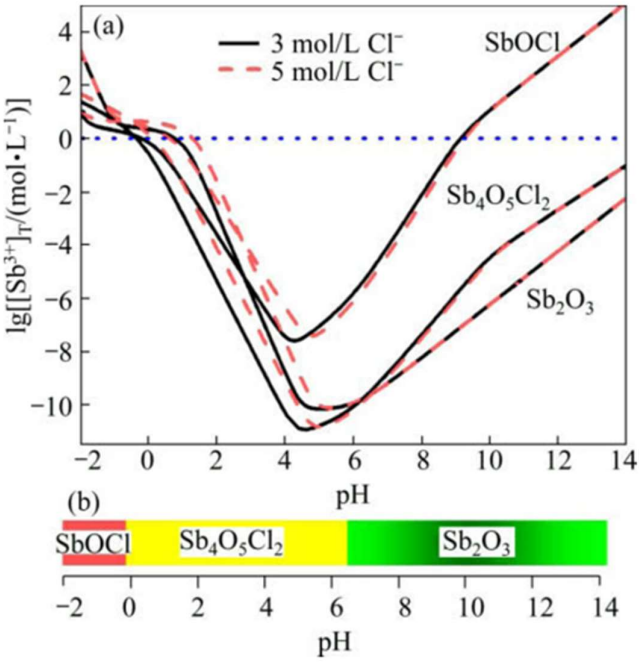

Figure 2:1: The stability interval of the generated compounds and lg[Sb^{3+}]-pH curves of antimony.

Sb precipitates in the form of SbOCl when the pH is under the value -0.2. Precipitation interval for $Sb_4O_5C1_2$ is between pH -0.2 and 6.6. Over this value Sb_20_3 is generated. Studies on the hydrolysis balance of the Sb^{3+}-Cl-H_2O system are limited to theoretical data, and have not yet been confirmed by experimental studies. Due to some deficiencies in these theoretical analyzes, the control mechanisms of this system are not fully understood.

3. THEORY

3.1. Cementation of Antimony Using Metallic Zinc

Cementation reactions are heterogeneous electrochemical reactions that require electron transfer between precipitant and soluble metals. It is an old method that allows to separate metal ions from solution. The addition of a non-toxic, inexpensive and more active metal to the solution ensures that the more noble metal precipitates. The more noble metal is deposited on the surface of the active metal. Zinc, for example, is widely used as an active metal. Its reduction potential is higher than most metals and it can be easily recovered.

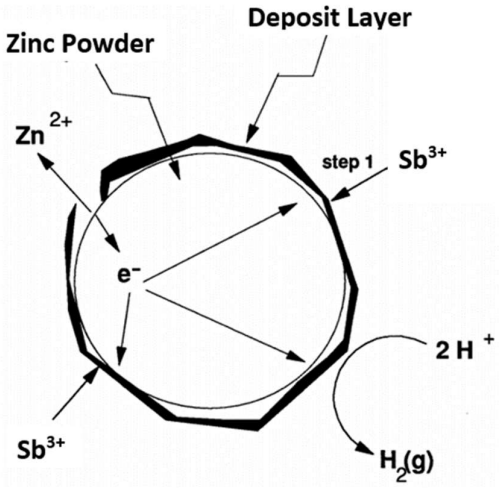

Figure 3:1: The schematic ilustration of a single zinc powder particle in the course of cementation process

Cementation is a multi-stage process. As illustrated in figure 2.2, the basic stages are as follows;

- Transfer of the atom to be cemented in solution to the active metal surface,
- Electron transfer from soluble metal to electroactive species,
- Separation of deposited metal from solution,
- Transport of metal ions through the sediment layer to the surface,
- Transfer of dissolved metal ions from surface to solution,

Equation 3.1 shows the cementation reaction in which case zinc is used as the reducing agent. Me is a metal which has a more positive reduction potential than zinc. In addition to antimony, metals like cadmium, iron, cobalt, nickel, arsenic, copper can also be obtained by cementation technique.

$$Me^{2+}(aq) + Zn(s) \leftrightarrow Me(s) + Zn^{2+}(aq) \quad (3.1)$$

Whether a metal in the solution can be cemented can be predicted by the standard reduction potential (E°). The potential difference between the standard reduction potentials and the standard hydrogen electrode (SHE) of the metals mentioned in this study and to be used in the experiments are given in Table 3.1.

Table 3.1: Selected standard reduction potentials in aqueous solutions at 25 °C vs. SHE [64].

Reduction half-reaction	Potential, E° (V) vs SHE
$Zn^{2+} + 2e^- \rightarrow Zn^o$	-0.762
$Sb^{3+} + 3e^- \rightarrow Sb^o$	0.208

It is expected that metals with a reduction potential less than zinc can be thermodynamically reduced by the addition of zinc powder. Due to the difference between antimony and zinc standard electrode potentials, zinc powder anodically dissolves and Sb^{3+} ions become neutral and precipitate. The Zn^{2+}/Zn system has more negative potential zinc in the first stage of cementation. Thus zinc dissolves easily. Therefore, antimony ions are reduced by cathodic reaction and the reaction takes place according to equation 3.2.

$$2Sb^{3+}(aq) + 3Zn^{\circ}(s) \rightarrow 2Sb^{\circ}(s) + 3Zn^{2+}(aq) \quad (3.2)$$

Reduction of antimony with oxidation of zinc causes a cell potential difference of 0.97 V. The potential difference is related to standard free energy (ΔG°) according to Equation 3.3.

$$\Delta G^{\circ} = -nFE^{\circ} \quad (3.3)$$

F and n are the Faraday constant and the number of electrons transferred in the oxidation-reduction reaction, respectively. E° is the standard potential of the chemical reaction given in Equation 3.2. When we replace the E(V) values in Table 3.1 in equation 3.3, the standard free energy of antimony cementation reaction can be calculated as G° = -561.63 k.Joule/mol. Due to the high negative G value, the precipitation of antimony from the solution with zinc can be predicted thermodynamically. It is a heterogeneous reaction and can be seen as a simple galvanic cell since it occurs spontaneously. During cementation, antimony deposits build up on the surface of the cementing agent. That is, the electron transfer from zinc to Sb^{3+} ions is transmitted through this deposit through a series of short electrochemical cells. Oxidation is possible in the anodic zones on the zinc surfaces.

$$\ln K_{eq} = -\frac{\Delta G^{\circ}}{RT^{\circ}} \quad (3.4)$$

From the standard free energy, the equilibrium constant K_{eq} is calculated as 2.4 x 10^{98} using Equation 3.4. By this value, it can be understand that the cementation reaction of antimony given in Equation 3.2 proceeds and reverse reaction is almost out of question. [65]. However, due to the increase in zinc, the cell potential decreases rapidly as the reaction progresses. After equilibrium, the potentials of two half cells (Zn/Zn^{2+} and Sb^{3+}/Sb) are equal. Hence at 25°C we have:

$$E^{\circ}_{Sb} + \frac{0.0591}{2} \log a_{Sb^{3+}} = E^{\circ}_{Zn} + \frac{0.0591}{2} \log a_{Zn^{2+}} \quad (3.5)$$

And, thus, we get;

$$\frac{a_{Sb^{3+}}}{a_{Zn^{2+}}} = 1.5 \times 10^{-33} = \frac{[Sb^{3+}]}{[Zn^{2+}]} \quad (3.6)$$

The low ratio of concentrations indicates a very low concentration of antimony ions remaining in the solution. As a result, antimony can be effectively recovered by cementing with zinc. [66]

The pH of the solution is one of the most important parameters of the cementation process. According to Equation 3.7, the pH of the solution increases with the addition of zinc dust.

If the pH of the solution rises, basic zinc salts such as $Zn(OH)_2$ may precipitate. At the same time, hydrogen gas is released according to equation 3.7.

$$Zn^{\circ}(s) + 2H_2O \rightarrow Zn^{2+}(aq) + 2OH^{-}(aq) + H_2(g) \quad (3.7)$$

The mass transfer coefficient of hydrogen is higher than zinc. As a result, zinc concentration increase in the surrounding layer on the zinc powder more than the concentration of hydrogen. Zn^{2+} ions in the layer lead to a charge imbalance. This charge is balanced by possible anions (hydroxyl ions). [67] This raises the pH locally and causes precipitation of basic salts such as ZnO or $Zn(OH)_2$. These salts formed on the surface of the zinc powder particle can block the active zinc surface required for cementation and cause a significant decrease in yield. Increasing the temperature increases the reaction kinetics. [68] In this case, the antimony present in the solution is expected to cement out of the solution more rapidly.

4. MATERIALS & METHODS

4.1. Materials Used in the Experiments

Antimony (III) chloride (≥99%, Sigma Aldrich)

Zinc powder (P80: 150 µm, Aldrich)

Tartaric acid (Merck)

Hydrochloric acid (Merck)

Sodium Bromate (≥99%, Sigma Aldrich)

Sodium Bromide (≥99%, Sigma Aldrich)

4.2. Process Layout of Experiments

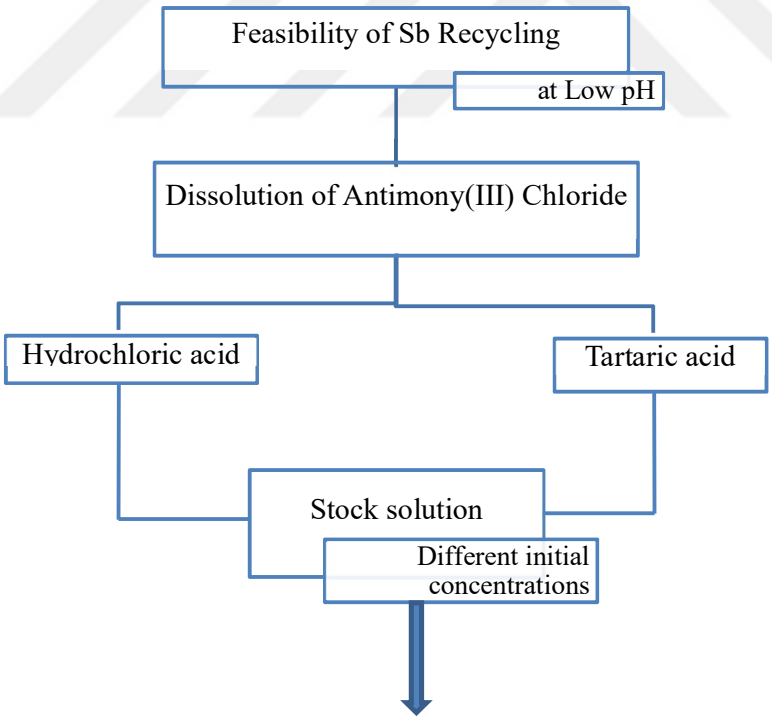

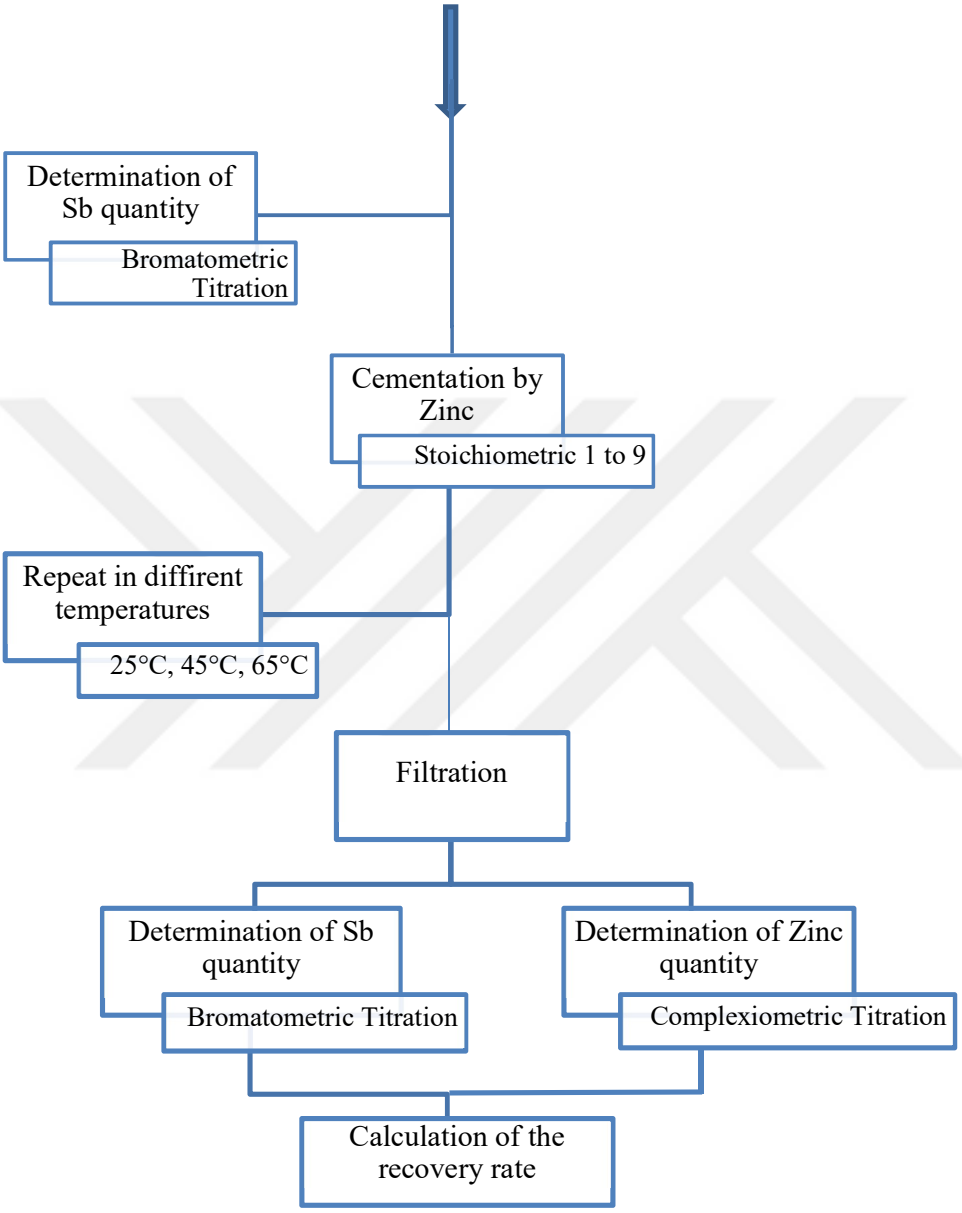

Figure 4:1: Flow sheet of the applied process

As it was seen in Figure 4.1, the applied process flow diagram was summarized briefly. All chemicals used were of analytical grade and was weighed on the precision balance to ensure high accuracy.

4.3. Dissolution of Antimony(III) Chloride

Antimony (III) chloride was selected as the initial antimony compound. A study on dissolution of $SbCl_3$ was done using tartaric acid (Merck) and hydrochloric acid (Merck).

Tartaric acid is fully soluble in aqueous solution, which binds and dissolves antimony compounds in the pH range 2-4. It makes a stable complex with antimony. Because the antimony tartrate complex has less negative potential than hydrogen in the solution. and prevents hydrolysis of $SbCl_3$. It was found that minimum 10 g/L tartaric acid must be added to dissolve $SbCl_3$ completely to obtain 1000 ppm $Sb3^+$. Apart from the tartaric acid, solubility of $SbCl_3$ in the hydrochloric acid was investigated. It was noticed that minimum 3M or higher concentration of HCl is required for complete dissolution of $SbCl_3$.

Consequently, 10 g / L tartaric acid (Merck) was dissolved in the mixing solution using a magnetic stirrer. In one experimental group, hydrochloric acid solutions of 3M and 4M were prepared without tartaric acid. The amount of dissolved Sb^{3+} was determined with bromatometric titration method. It was approved that the purity of $SbCl_3$ was in the range of %99.5±0.5.

4.4. Determination of Antimony Concentration

The yield of antimony (III) ions in the stock solution and the yield of the antimony (III) ions remaining in the processed solutions after cementation were determined by utilizing bromatometric titration method through an Automatic titrator (TitroLine® 6000 Easy Titrator) with the combination of Ag/AgCl reference electrode and a platinum indicator electrode.(Figure 4.2) 0.005M Sodium Bromate, $NaBrO_3$ was used as primary grade titrant. To dissolve chemicals, de-ionized water was employed (Direct-QTM 5 system; Millipore). All the sample solutions were diluted with 3M hydrochloric acid.

Figure 4:2: Titration of the stock solution through automatic titrator before cementation process.

After a range of trials, optimum stability and accuracy were obtained with the parameter in Table 4.1.

Table 4.1: Optimum settings for Sb^{3+} titration in automatic titrator.

Parameter	Settings
Titration Mode	Dynamic
Titration direction	Increasing
Measurement time	2 second
Drift	10 mV/min
Min. time	3 second
Max time	15 second
Dosing speed	20 %
Dynamics	Average
End criterion	1 EQ
Slope value	300 mV/mL
End point delay	5 second

Titration signals were unstable and noisy when the concentration of antimony is above 1000 ppm. In order to maintain accuracy of the results, incremental titrant addition mode was performed for these samples.

Volumetric method was used for calibration purpose. First the concentration of the titrant was confirmed and then used in the auto titration process. The sample solutions were transferred only with calibrated piston-stroke pipettes. To measure the pH of the sample, HI2002-01edge® Dedicated pH/ORP Meter and wireless pH electrode were used. (Figure 4.3) Before measurements, the pH electrode was calibrated through standard reference solutions with pH values of 4, 7, and 10.

Figure 4:3: pH measurement after solid/liquid separation

4.4.1. Bromatometric Titration Method

Bromatometric titrations are carried out in an acidic medium in the presence of halide ions, such as bromide or chloride. In this case, the following reactions occur, depending on the actual concentration of bromate, bromide and chloride:

$$BrO_3^- + 5Br^- + 6H^+ \rightarrow 3Br_2 + 3H_2O \quad (4.2)$$

$$BrO_3^- + 2Br^- + 3Cl^- + 6H^+ \rightarrow 3BrCl + 3H_2O \quad (4.3)$$

$$BrO_3^- + 5Cl^- + 6H^+ \rightarrow BrCl + 2Cl_2 + 3H_2O \quad (4.4)$$

According to Equation 4.2, bromine forms in presence of excess bromide. Equation 4.3 shows that bromine chloride forms in the presence of chloride, while elementary chlorine and bromine chloride forms in the absence of bromide as shown in Equation 4.4. [69]

In bromatometric titrations, oxidizing agents can be bromine, elementary bromine or mixture of bromine chloride and elementary chlorine. Conventional brometric titrations are usually performed in bromide or hydrochloric acid containing solutions. Free bromine appears at the end point of titration, according to main Equation 4.5 of bromatometry; [70]

$$NaBrO_3 + 5Br^- + 6HCl \rightarrow 3Br_2 + 6NaCl + 3H_2O \quad (4.5)$$

4.5. Production and Characterization of Metallic Antimony

In each experiment, zinc powder, stoichiometric multiples of the amount of antimony, was used to precipitate the antimony in the solution. Each time stock antimony solution of 25 mL by the addition of zinc powder was transferred to volume centrifuge tubes of 50 mL. Experimental study was carried out in a temperature controlled water bath in order to ensure temperature control, uniform temperature distribution and uniform heat convection.(Figure 4.4-4.5) All samples except the control group were shaken for 5 hours at the specified constant temperature. The experimental procedure was repeated three times, using separate arbitration specimens in each run. After each cementation experiment, solid/liquid separation was performed using filter paper (Blue band, Sartorius,). The solid product was rinsed with acetone and dried in a vacuum drying oven system at 50°C.

Figure 4:4: Water bath unit with temperature and shaking control system

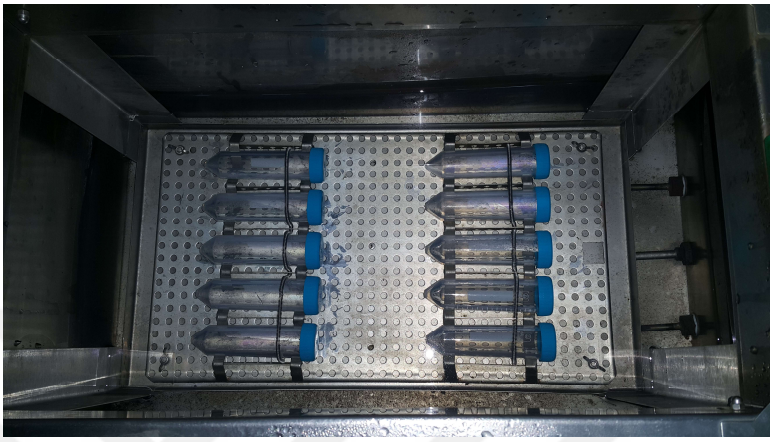

Figure 4:5: Zinc added solution samples on the modified shaking system of the water bath unit

The recovery efficiency (%) of this cementation process was calculated using the following equation:

$$\text{Recovery}(\%) = \left[\frac{(C_0 - C_t)}{C_0}\right] \times 100 \qquad (4.1)$$

wherein C_0; the initial antimony concentration and C_t are the final antimony concentration at the end of the experiment.

The results of each sample were compared graphically after measurement. XRD measurements of antimony metallic powder after cementation were carried out using Rigaku vertical diffractometer with Cu Kα radiation by step size of 0.02◦ (2θ) with 2 second intervals under conditions of 40 mA and 40 kV. The phases of the diffraction pattern were determined using the JADE 6 program. The purity of the product was evaluated through Niton™ XL2 X-Ray Fluorescence spectrometer with SDD Silicon Drift Detector. The surface morphology and microstructure of the cementation product was analyzed through FEI Sirion XL30 scanning electron microscope with an integrated Oxford Inca energy dispersive X-ray detector (EDX).

4.6. Determination of Zinc Concentration

After cementation, the amount of dissolved zinc was determined using complexometric titration method with 0.01 M EDTA solution. Titration was performed at pH 10 since EDTA chelates perfectly with zinc and forms a stable complex. A metallochromic indicator (Eriochrome Black T) was used with ammoniacal buffer ($NH_4Cl + NH_3$) which is called as Schwarzenbach's buffer(570 ml of concentrated ammonia solution per liter + 70 g of ammonium chloride). Color transition was quite sharp at pH-10 from wine red to blue.

Figure 4:6: Determination of the zinc content after cementation

Analytical grade disodium EDTA(Y), $Na_2H_2Y.2H_2O$ was standardized by using zinc sulphate ($ZnSO_4.7H_2O$) as recommended in literature. Both chemicals contains hygroscopic water and were dried by using a vacuum drying oven system (Figure 4.7).

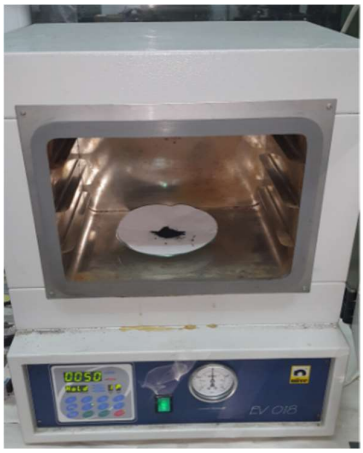

Figure 4:7: Metallic antimony powder dried in the drying oven

5. RESULTS and DISCUSSION

5.1. Effects of Parameters on Cementation Efficiency

To investigate the cementation behavior of antimony in acidic medium, two types of stock solution were used. Tartaric acid and hydrochloric acid were known to be able to to dissolve %100 of $SbCl_3$ in literature. This condition was confirmed experimentally for various concentration of $SbCl_3$ solution. In the following section, parameters effecting cementation efficiency were addressed in detail.

5.1.1. Effect of zinc quantity

Figure 5.1 shows that recovery(%) of antimony with increasing amount of metallic zinc powder. Each measurement point in diagrams represents a cementation experiment for given amount of zinc with repetition number of three. Stock solution initially contained antimony ions of 1000 ppm. Same cementation experiment was iterated at temperatures of 25°C, 45°C and 65°C.

The recovery was nearly complete when zinc powder of 100 mg was used at 25°C. 20 mg of zinc corresponds stoichiometrically to the antimony of 1:1 and zinc additions were performed stoichiometrically. Similarly, stoichiometric 1, 3, 5, 7 and 9 correspond to the specific amount of zinc of 20, 60, 100, 140 and 180 mg, respectively. By increasing the amount of active metal to be used in cementation, here is, increasing the amount of zinc per antimony ion, the surface area at interaction and the percentage yield of metallic antimony was increased [71-72]. In similar cementation studies, it has been observed that increasing the amount of zinc as active metal increases the percent yield of silver cementation [27].

As the zinc powder was consumed by the acidic medium rather than used for the cementation, in some experiments even more than 4 times of the stoichiometric ratio of the zinc powder was not sufficient to recover the whole antimony present in the sample.

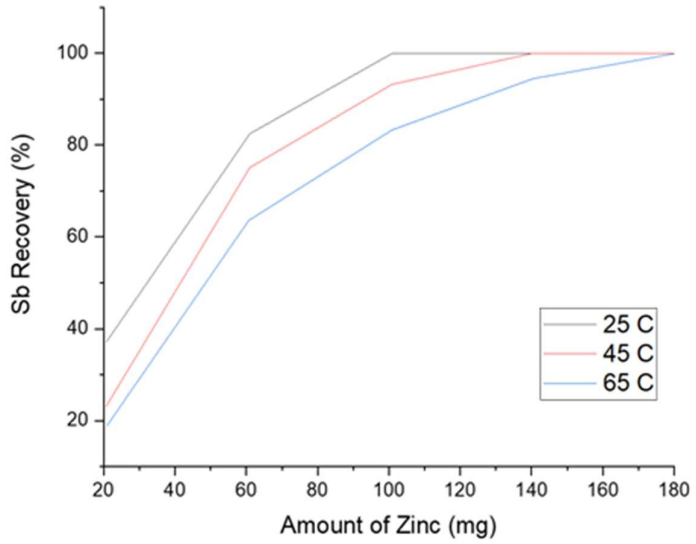

Figure 5:1: Relation between antimony recovery and increasing amount of zinc at different temperatures. (25mL, 1000ppm Sb3+, 10g/L Tartaric acid, 60 rpm, 5 minutes)

5.1.2. Effect of temperature

Figure 5.1 also shows the relation between Sb recovery (%) and temperature based upon zinc amount. 65°C was chosen as maximum temperature due to the volatile nature of antimony compounds. Efficiency in cementation reactions is expected to increase with temperature in general. However, it was determined that the temperature had a negative effect during the cementation process of antimony (III) ions with zinc. The negative effect of temperature on yield may be explained as follows:

- Increasing the rate of hydrogen gas production on the zinc surface and consequently complicating the displacement reaction of zinc with antimony
- Preferential re-dissolution of the precipitated antimony in the presence of tartaric acid at elevated temperatures [73-74].
- Increasing the affinity of the acid to Zn metal with increasing temperature compared to antimony ions preferentially dissolves the zinc in the acid solution without cementing out.

Another reason can be attributed to the fact that antimony ions block zinc dust particles in early stage of cementation to inhibit further reaction. Cementation kinetics increases with temperature, Sb ions become more active and block zinc early. This blockage effect may prevent cementation reaction. So the recovery is lower for 65°C than that of 45°C and 25°C.

5.1.3. Effect of reaction time

Figure 5.2 shows the antimony recovery efficiency over time. Approximately 20 mg of zinc is stoichiometrically sufficient for cementation of all antimony in 25 mL of sample solution in theory. While the recovery efficiency increased dramatically up to the first 5 minutes, it approached zero with a decreasing trend after 5 minutes. After 5 minutes at 25°C, 39% antimony was recovered in solution while the amount of recovery decreased to 4% at 15 minutes. During cementation, decrease in precipitated metallic antimony powder was observed visually. It can only be explained that cemented antimony re-dissolved in acidic medium in the presence of tartaric acid. Free acid in the solution helps precipitated antimony to dissolve again as time passed by.

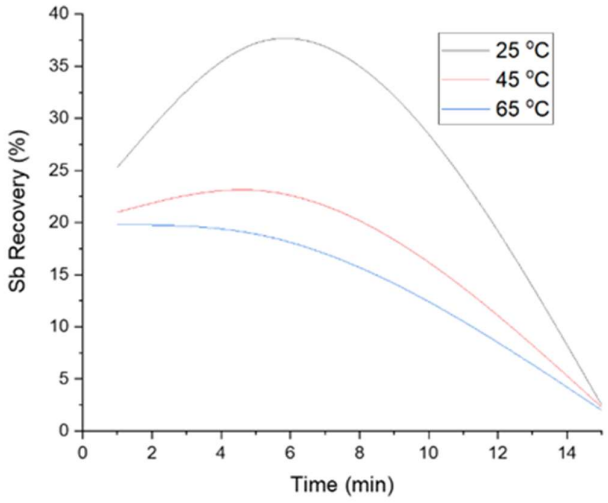

Figure 5:2: Relation between antimony recovery and reaction time at different temperatures. (25mL, 1000ppm Sb3+, 10g/L Tartaric acid, shake, Stoichiometric ratio x1)

In Figures 5.2 and 5.3, there are two interesting stages: The first stage, which takes place between 0 and 5 minutes, represents the cementation of the antimony and the dissolution of the zinc powder to the solution, while the second stage, i.e. after the 5th minute, the antimony cementation and the zinc-coupled antimony back-dissolution.

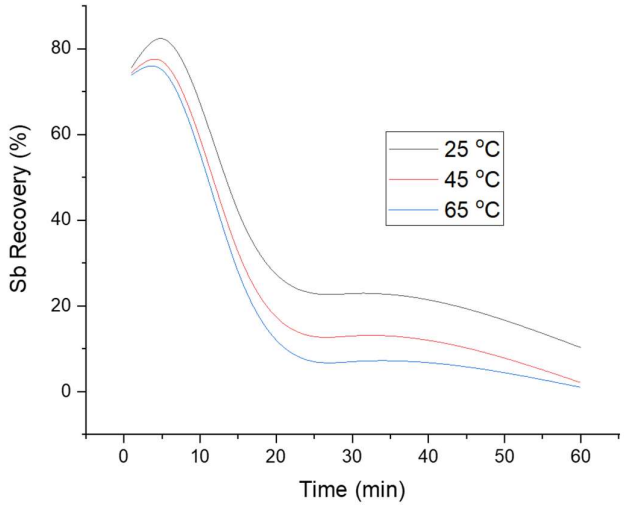

Figure 5:3: Relation between antimony recovery and reaction time at different temperatures. (25mL, 1000ppm Sb3+, 10g/L Tartaric acid, 60 rpm, Stoichiometric Ratio x3)

Referring to Fig. 5.4, the stoichiometric 1, 3 and 5 samples showed a dramatic change in the amount of antimony recovery with increasing amount, while the changes were similar after the 5th minute following the addition of stoichiometric 5 sample. Significant difference was reached in the stoichiometric 9, and the antimony cementation with 100% antimony recovery efficiency was achieved with the antimony cementation. Since the stoichiometric 9 contained much more zinc than necessary, it first precipitated the antimony, then the antimony paired with the zinc was reintroduced, but since there was still too much zinc in the system, the cementation resumed and almost 100 % of cementation efficiency was obtained. Of course, due to the acidic environment, zinc was preferentially consumed by acid.

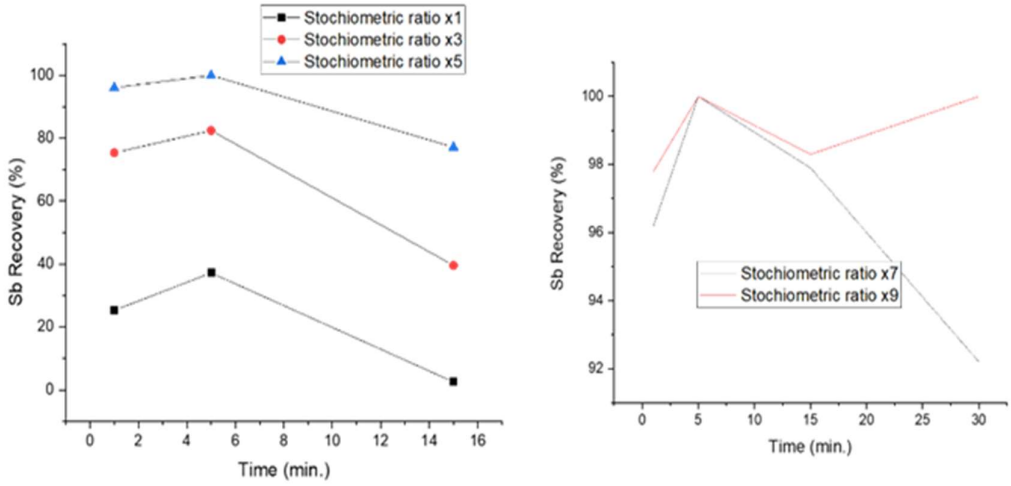

Figure 5:4: Comparison of the alteration in antimony recovery(%) with various amounts of zinc at constant temperature. (25mL, 1000ppm Sb3+, 10g/L Tartaric acid, 60 rpm, 25°C)

In the experiments with different concentration of HCl, it was found that minimum 3M HCl is required to dissolve 0.2M $SbCl_3$. In the course of HCl, zinc also reacts with free acid and hydrogen gas released. This increased the pH of the solution. As a result, the more zinc added to the system, the more pH of the system increased. This result can be seen in Figure 5.5. At fifth minute the recovery was 32% and 26% at the end of second hour. Only 6% decrease was occurred because of re-dissolution. The difference is significant in comparison with tartaric acid containing stock solutions. An optimum point at minute-5 was out of question with the cementation using HCl. As a consequence, results were more stable.

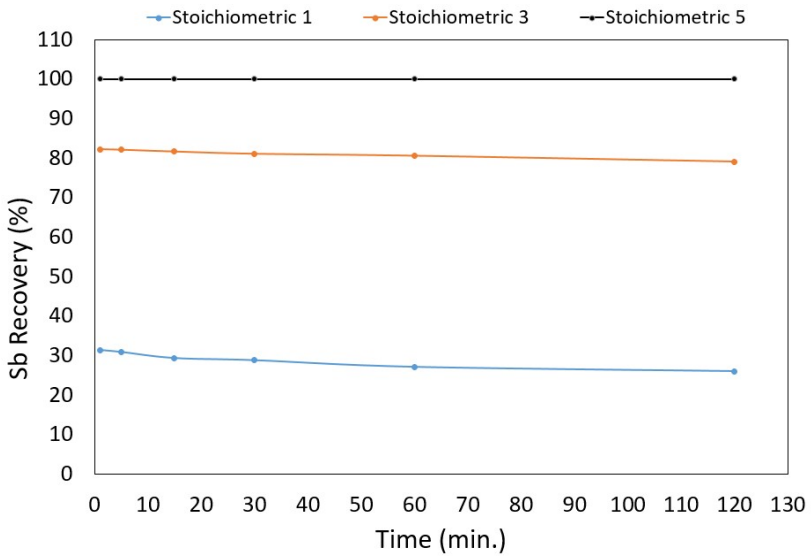

Figure 5:5: The change in antimony recovery(%) with various amounts of zinc at constant temperature. (25mL, 0.2M Sb3+, 3M HCl, 60 rpm, 25°C)

5.1.4. Effect of initial concentration

1000ppm Sb^{3+} concentration can be considered high when compared with industrial waste solutions. To see the behavior of antimony at low concentrations, same experiments was performed at 500 ppm and 100 ppm solutions. In Figure 5.6, it is clear that recovery efficiency is directly proportional with initial concentration of antimony in stock solution. It can be concluded that if the concentration of Sb^{3+} ions increased, the chance of interaction of Sb^{3+} and Zn^{2+} ions increases.

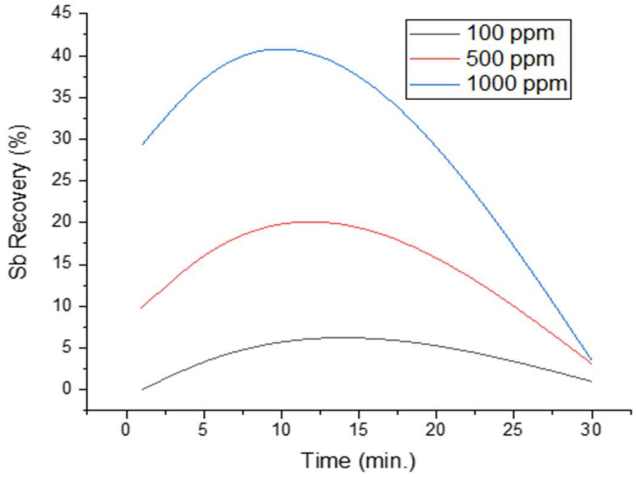

Figure 5:6: The ratio of dissolved zinc to the total amount of zinc added. (10g/L Tartaric acid, 60 rpm, 25°C, Stoichiometric x1)

The amount of dissolved zinc began to decrease significantly from the stoichiometric-5 as in Figure 5.7. This means that almost all free acid is neutralized with metallic zinc. Following the neutralization, white precipitates (Figure 5.8) were formed due to hydrolysis and formation of basic zinc salts.

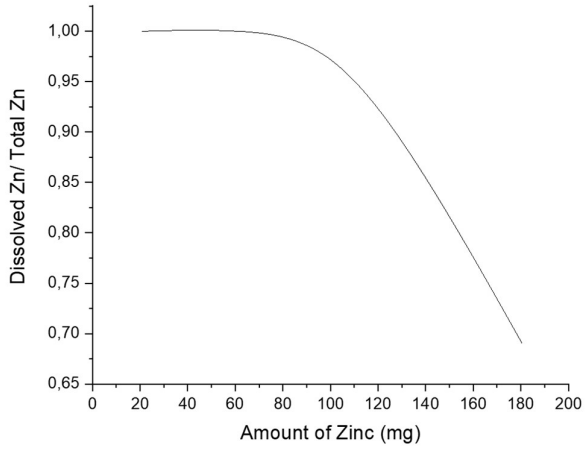

Figure 5:7: The degrees of dissolved zinc (mg) with different amounts of zinc added to the solution (25mL, 1000ppm Sb3+, 10g/L Tartaric acid, 60 rpm, 120 minute, 25C)

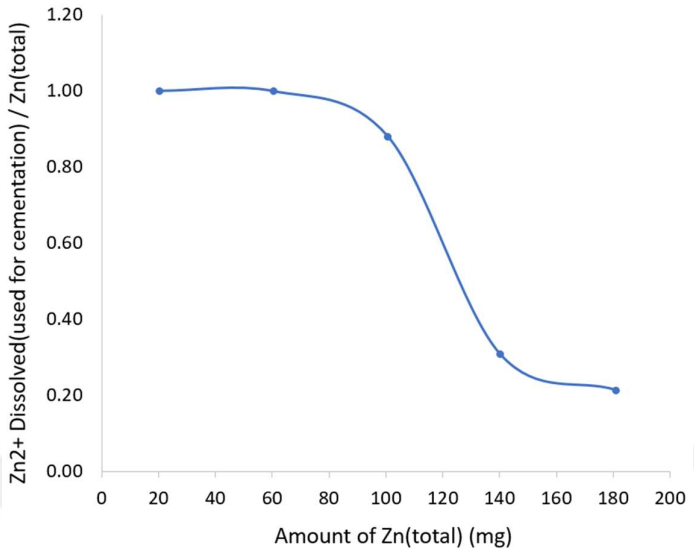

Figure 5:8: The degrees of dissolved zinc(mg) only used for cementation with different amounts of zinc added to the solution (25mL, 1000ppm Sb3+, 10g/L Tartaric acid, 60 rpm, 120 minute, 25C)

Figure 5:9: Precipitated form of zinc hydroxide after cementation

5.1.5. Effect of shaking speed

As shown in Figure 5.9, shaking of the sample solution improves the yield of the cementation significantly. Although a recovery of 38% was achieved using shaking at 5 minutes, it was 31% without shaking.

But shaking also expedited redissolution of the cemented antimony. Without shaking, it took time to reach maximum efficiency and redissolution started at 60th minute.

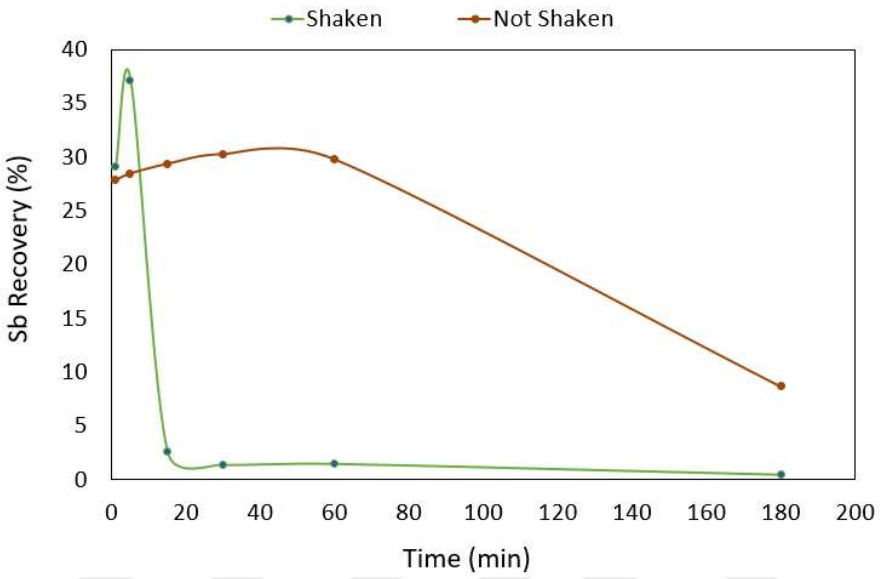

Figure 5:10: The effect of shaking and stirring on the cementation of antimony at constant temperature. (25mL, 1000ppm Sb3+, 10g/L Tartaric acid, 60 rpm, 25°C, Stoichiometric x1)

5.2. Optimization Studies to Increase Cementation Efficiency

A study on the addition of zinc powder in two steps aimed to improve the amount of cemented antimony by reducing the amount of zinc. At first step, 40mg (stoichiometrically 2 times) zinc powder was loaded to the stock solution sample. At the end of 5 minutes, %59.1 of total antimony in the solution was precipitated as metallic antimony. After the first cementation, the solution was filtered and product was seperated. To the remaining solution stoichiometrically 2 times zinc was loaded again and cementation was repeated along 5 minutes. As a consequence, when 100% recovery was achieved with 100 mg Zn in single-stage cementation, the same yield was achieved with the addition of 40% less zinc in two-stage cementation as shown in Fig. 5.10.

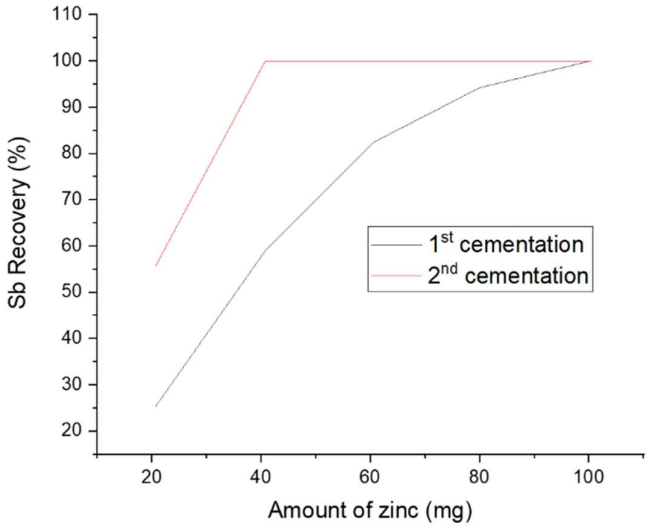

Figure 5:11: Comparison of one step and two step cementation in the basis of Sb recovery (25mL, 1000 ppm Sb3+, 3M HCl and 10g / L tartaric acid, 60 rpm, 5 minutes).

5.3. Characterization of the Cementation Product

For the characterization purpose, the sample was produced with the parameters yielding maximum output. According to experiments above, 0.2M Sb^{3+} in 3M HCl yielded the optimum cementation performance of which the result was shown in Figure 5.5. The metallic antimony powder was treated with acetone and dried under vacuum at 60 °C for 1 h. The product was found to contain 99.2% ± 0.8 antimony and 0.3% ± 0.02 zinc as shown in the XRF analyses. (Figure 5.11). This result was also matched with the titration results of the processed solution

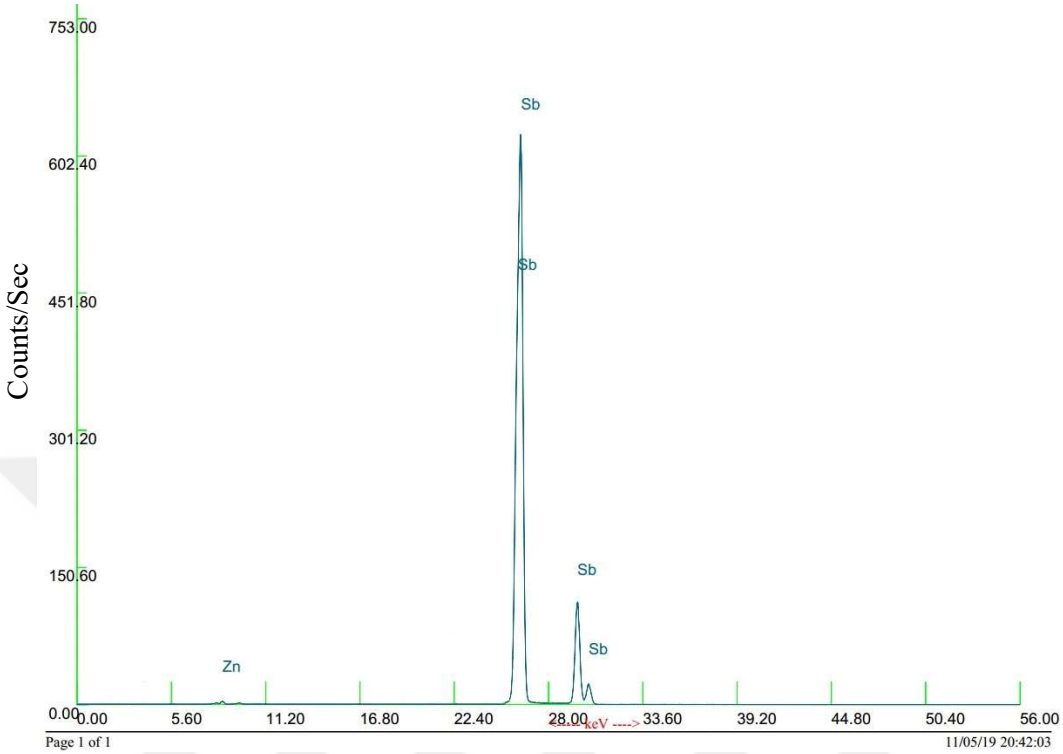

Figure 5:12: The result of XRF analysis in general metals mode with acquisition time of 61s.

XRD results of the antimony powder produced with the same reaction conditions (0.2M Sb^{3+} in 3M HCl) confirmed the result of XRF analysis. In figure 5.12, all diffraction peaks belong to antimony metal and available as single phase antimony.

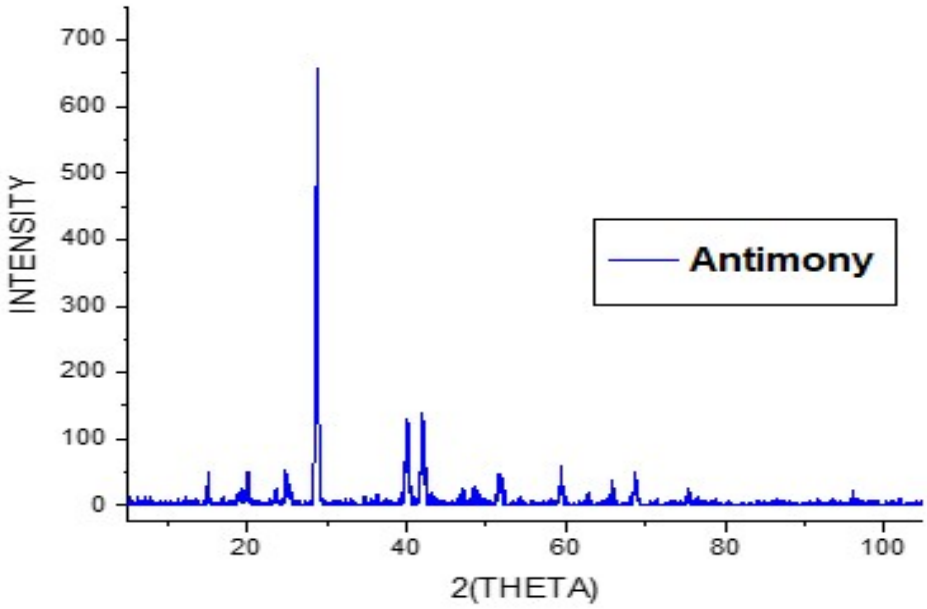

Figure 5:13: The XRD diffraction pattern of antimony powder cemented through stoichiometrically 5 times zinc addition.

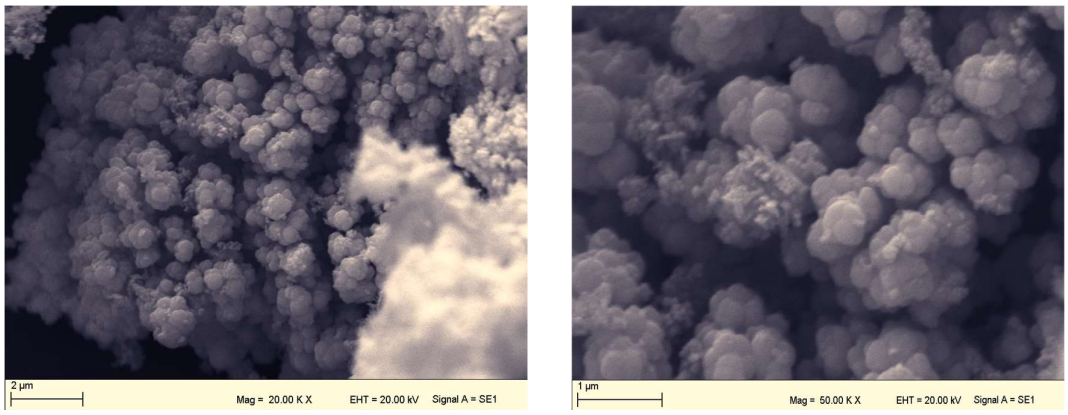

Figure 5:14: SEM image of the antimony powder obtained through cementation by zinc powder. (25mL, 3M HCl, 60 rpm, 25°C, 5 minute)

The powder structure is mostly nodular, agglomerated and less than one micron. During treatment, the remnants of the acetone may cause the agglomeration of particles.

To compare the effect of pH on the cementation product, another antimony sample produced with same concentration (0.2M Sb^{3+}) but lower acidity (2M HCl). Again cementation residues were collected at the end of 5 minutes. This time the grains were greater in size (Figure 5.14) in comparison with the previous sample displayed in Figure 5.13. Their shape was twiggy and spherelike and their surface was covered with more deposit.

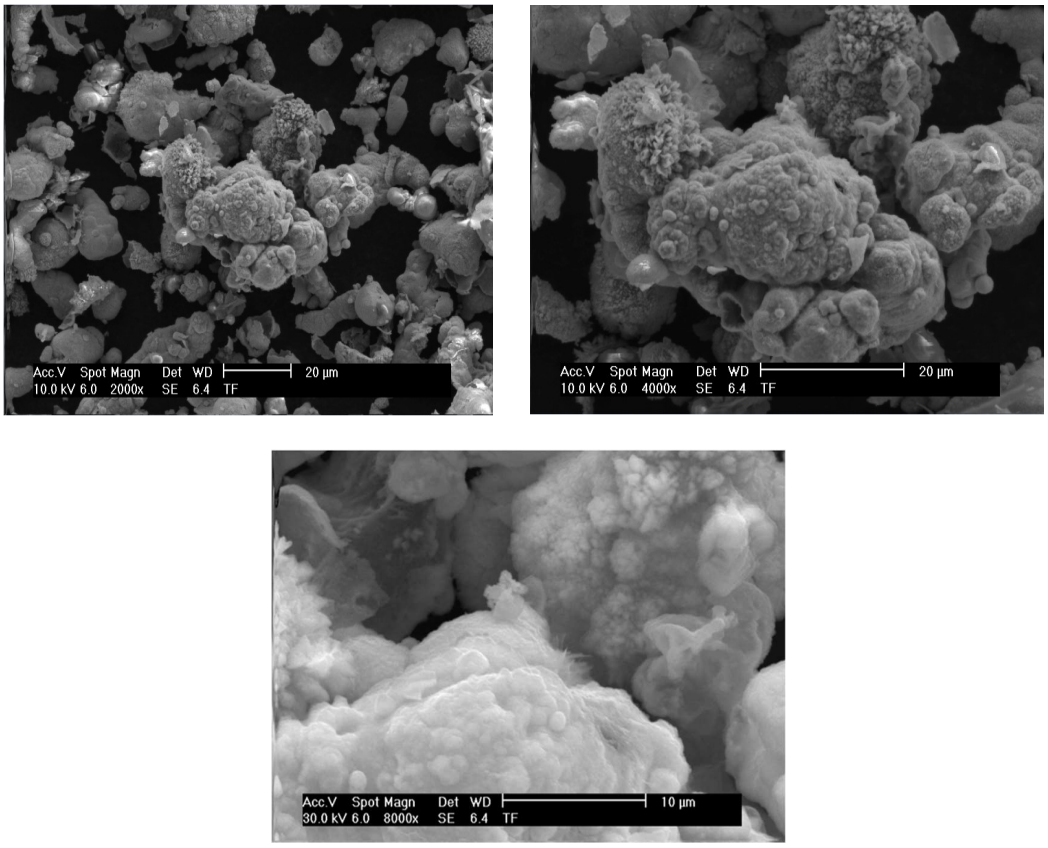

Figure 5:15: SEM image of the metallic antimony powder gained through cementation by zinc powder. (25mL, 2M HCl, 60 rpm, 25°C, 5 minute)

While the zinc dust dissolved during cementation, hydrogen was produced in the gas form. As hydrogen gas evolves, localized pH around the active sites of the zinc powder increases and cause the formation of zinc hydroxide. In Figure 5.14, it can be seen as thin deposit layer (mossy and platelet) surrounding the zinc powders. This layer passivates the surface of the zinc powder and retards antimony cementation. In addition, zinc powders found among cemented antimony powders continue to dissolve.

Zinc release electrons during its dissolution, which are consumed by protons in the electrolyte and lower the reduction of antimony. Thus, the significant amount of cathodic current is consumed by the hydrogen evolution during cementation.

According to Van der Pas and Dreisinger [65], it is proven that purity up to 98 % is possible. As a result of this detrimental reaction, pH increased and lead to zinc hydroxide formation which resulted in the inhibition of antimony removal. Inhibition effect of these passivating substances is observed when the pH is relatively high.

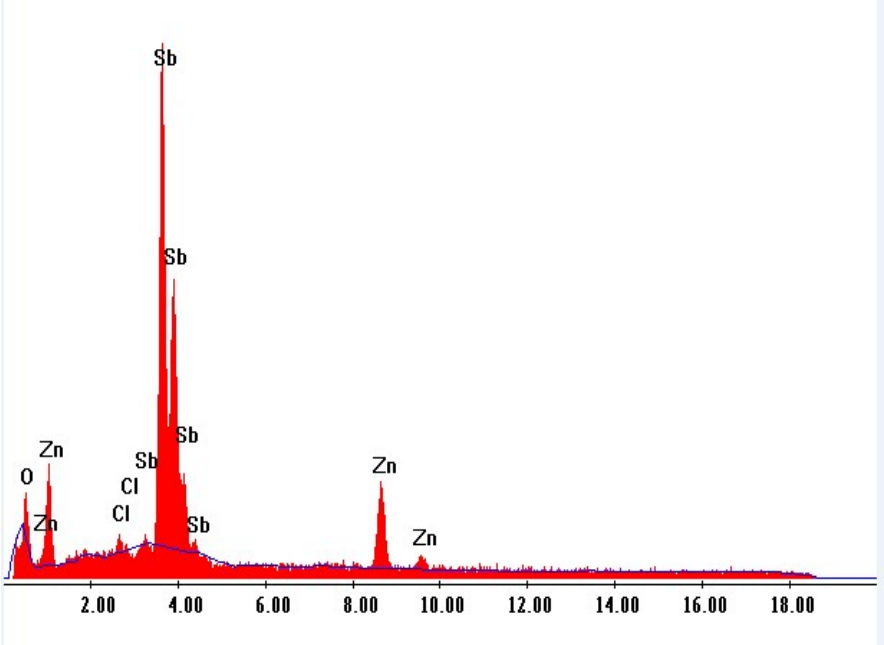

Figure 5:16: SEM-EDS diagram of the antimony powder gained through cementation by zinc powder. (2M HCl, 60 rpm, 25°C, 5 minute)

Processing option: All elements analyzed (Normalized)

Element	Sb	Zn	O	Cl
Spectrum	75.83	14.34	8.43	1.40

The result confirms the formation of zinc hydroxide on the zinc dust surface. The formation of zinc hydroxide is not the only reason for inhibition. Zinc ions surrounding the zinc powder cause repulsion against Sb^{3+} ions. This effect depends on the level of zinc ions.

6. CONCLUSIONS

Generally, the primary antimony production is limited to a few countries and mostly dominated by China. Therefore, antimony is currently considered as a strategic material. The metallurgical methods used in production are wide spread. This study aims to find out if recovery of antimony could be possible hydrometallurgically from acidic solutions since recycled amount of antimony is limited today. The results obtained with cementation technique provided evidence for this phenomenon.

Initially the concentration of the solution was determined in order to quantify the solubility of antimony chloride. It was found that high quantities of zinc powder was required to recover more than 99% of the antimony metal, which is proved by pH measurements and concentration analyses.

Inhibition of zinc dust and blockage effect of antimony ions decreased recovery performance. By the increase in temperature, these effects became more significant, and recovery (%) decreased more which is interesting. The contribution of shaking to efficiency (%) was also limited. It only increased 8% for the stoichiometric-1 at 25°C and also increased the redissolution of cemented antimony which is undesired. It was seen that an optimum reaction time is the point in question. At each temperature, the cemented Sb started to re-dissolve after 5 minutes of the reaction thus lowering the cementation efficiency. It can be suggested that cementation must be terminated at fifth minutes of the reaction.

In a separate study, residue morphology of zinc hydroxides and zinc chloride formation was investigated. It was shown that these salts forms a passivating layer retarding antimony removal. This is because the evolution of hydrogen creates a localized high pH. Hydrogen evolution accordingly increase in pH continues until complete dissolution of zinc dust particles. When the generation of hydrogen stops, pH reach a plateau. Avoiding the formation of the salts may improve the recovery performance, however, it could not be possible using the parameters studied in this present work.

The results showed that antimony recovery through cementation process can be applicable in large scale industry. The main cement product i.e. 99% purity antimony meets the requirements of the electronic industry. In this project a non-hazardous

hydrometallurgical process was proposed. It avoids environmental problems and enables recovery of valuable antimony from antimony-containing waste solutions.

7. REFERENCES

1. Jha, M., Kumar, V., & Singh, R. (2001). Review of hydrometallurgical recovery of zinc from industrial wastes. Resources, Conservation and Recycling, 33(1), 1-22.
2. Chang, F., Lo, S., & Ko, C. (2007). Recovery of copper and chelating agents from sludge extracting solutions. Separation and Purification Technology, 53(1), 49-56.
3. Nosier, S., Sallam, S., (2000). Removal of lead ions from wastewater by cementation on a gas-sparged zinc cylinder. Separation and Purification Technology, 18(2), 93-101.
4. El Batouti, M. (2003). Cementation reactions in the presence of nitrogen compounds. Journal of Colloid and Interface Science, 263(2), 548-553.
5. Dib, A., & Makhloufi, L. (2004). Cementation treatment of copper in wastewater: mass transfer in a fixed bed of iron spheres. Chemical Engineering and Processing: Process Intensification, 43(10), 1265-1273.
6. Fouad, O., & Abdel Basir, S. (2005). Cementation-induced recovery of self-assembled ultrafine copper powders from spent etching solutions of printed circuit boards. Powder Technology, 159(3), 127-134.
7. Mok, W.M., Wai, C.M. (1990) Distribution and mobilization of arsenic and antimony species in the Coeur d'Alene River, Environmental Science & Technology, 24, 102-108.
8. Guo, X., Wu, Z., He, M., Meng, X., Jin, X., Qiu, N., Zhang, J. (2014). Adsorption of antimony onto iron oxyhydroxides: Adsorption behavior and surface structure. Journal of Hazardous Materials, 276, 339-345.
9. Shan, C., Ma, Z., & Tong, M. (2014). Efficient removal of trace antimony(III) through adsorption by hematite modified magnetic nanoparticles. Journal of Hazardous Materials, 268, 229-236.
10. Wang, L., Wan, C., Zhang, Y., Lee, D., Liu, X., Chen, X., & Tay, J. (2015). Mechanism of enhanced Sb(V) removal from aqueous solution using chemically modified aerobic granules. Journal of Hazardous Materials, 284, 43-49.

11. Zhang, Z., Zhao, Y.B., Liu, R.Y., (2002). An experimental study on using micro-electrolysis-neutralization sedimentation process to treat the acidic mine underground. Nonferrous Metalurgy, 2, 45–47.

12. Kang, M., Kawasaki, M., Tamada, S., Kamei, T., & Magara, Y. (2000). Effect of pH on the removal of arsenic and antimony using reverse osmosis membranes. Desalination, 131(1-3), 293-298.

13. Wang, J.L., Chen, C., (2010). Research advances in heavy metal removal by biosorption. Acta Scientiarum Circumstantia, 30, 673–701.

14. Wu, F., Sun, F., Wu, S., Yan, Y., & Xing, B. (2012). Removal of antimony(III) from aqueous solution by freshwater cyanobacteria Microcystis biomass. Chemical Engineering Journal, 183, 172-179.

15. Kameda, T., Nakamura, M., & Yoshioka, T. (2012). Removal of antimonate ions from an aqueous solution by anion exchange with magnesium–aluminum layered double hydroxide and the formation of a brandholzite-like structure. Journal of Environmental Science and Health, Part A, 47(8), 1146-1151.

16. Zhu, J., Wu, F., Pan, X., Guo, J., Wen, D. (2011). Removal of antimony from antimony mine flotation wastewater by electrocoagulation with aluminum electrodes. Journal of Environmental Sciences, 23(7), 1066-1071.

17. Guo, X., Wu, Z., He, M. (2009). Removal of antimony(V) and antimony(III) from drinking water by coagulation–flocculation–sedimentation (CFS). Water Research, 43(17), 4327-4335.

18. Bergmann, M. H., & Koparal, A. S. (2011). Electrochemical antimony removal from accumulator acid: Results from removal trials in laboratory cells. Journal of Hazardous Materials, 196, 59-65.

19. Wu, L., Li, Y., Cao, H., & Zheng, G. (2015). Copper-promoted cementation of antimony in hydrochloric acid system: A green protocol. Journal of Hazardous Materials, 299, 520-528.

20. Habashi, F. (2005). A short history of hydrometallurgy. Hydrometallurgy, 79, 15–22.

21. Doyle, F.M. (2005). Teaching and learning environmental hydrometallurgy. Hydrometallurgy, 79, 1–14.

22. Aktas, S. (2011). Rhodium recovery from rhodium-containing waste rinsing water via cementation using zinc powder. Hydrometallurgy, 106, 71–75.

23. Syed, S. (2012). Recovery of gold from secondary sources-A review. Hydrometallurgy, 115-116, 30-51.

24. Sulka, G., & Jaskuła, M. (2004). Study of the mechanism of silver ions cementation onto copper from acidic sulphate solutions and the morphology of the silver deposit. Hydrometallurgy, 72(1-2), 93-110.

25. Power, G., Ritchie, I. (1976). A contribution to the theory of cementation (metal displacement) reactions. Australian Journal of Chemistry, 29(4), 699.

26. Demirkıran, N., Ekmekyapar, A., Künkül, A., Baysar, A. (2007). A kinetic study of copper cementation with zinc in aqueous solutions. International Journal of Mineral Processing, 82(2), 80-85.

27. Farahmand, F., Moradkhani, D., Sadegh Safarzadeh, M., & Rashchi, F. (2009). Optimization and kinetics of the cementation of lead with aluminum powder. Hydrometallurgy, 98(1-2), 81-85.

28. Karavasteva, M. (2005). Kinetics and deposit morphology of copper cementation onto zinc, iron and aluminium. Hydrometallurgy, 76(1-2), 149-152.

29. Nadkarni, R.M.,Jelden, C.E., Bowles, K.C., Flanders, H.E., Wadsworth, M.E. (1967). A kinetic study of copper precipitation on iron-part1. Transactions of the Metallurgical Society of AIME, 239, 581-585.

30. MacKinnon, D., & Ingraham, T. (1970). Kinetics of Cu(II) cementation on a pure aluminum disc in acidic sulphate solutions. Canadian Metallurgical Quarterly, 9(3), 443-448.

31. MacKinnon, D., Ingraham, T., & Kerby, R. (1971). Copper cementation on nickel discs. Canadian Metallurgical Quarterly, 10(3), 165-169.

32. MacKinnon, D., & Ingraham, T. (1971). Copper cementation on aluminum canning sheet. Canadian Metallurgical Quarterly, 10(3), 197-201.

33. Masse, N. (1994). Effects of Temperature and Powder Morphologies on the Cementation Rate of Copper in Alkaline Zinc Solution. Journal of The Electrochemical Society, 141(3), 664.

34. Kanungo, M., Mishra, K., & Das, S. (2003). Study on morphology of copper deposited onto aluminium by immersion plating from an oxalate bath containing perchloric acid. Minerals Engineering, 16(12), 1383-1386.

35. Hung, Y. P. (2001). Recovery of Copper from Strong Chloride-based Solution. Journal of Applied Sciences, 5, 1328-1333.

36. Mitsunobu, S., Takahashi, Y., & Terada, Y. (2010). μ-XANES Evidence for the Reduction of Sb(V) to Sb(III) in Soil from Sb Mine Tailing. Environmental Science & Technology, 44(4), 1281-1287.

37. Lagowski, J.J., (2004). Chemistry: Foundations and Applications, 1st Edition., Macmillan Reference Inc., New York, USA

38. Grund, S.C., Hanusch, K., Breunig, J.A. (2006). “Antimony and Antimony Compounds” in Ullmann's Encyclopedia of Industrial Chemistry. Wiley-VCH, Weinheim.

39. Bernard, H.W., De Jong, S., Ruud, G.C., Beerkens, P. A. (2005). "Glass" in Ullmann's Encyclopedia of Industrial Chemistry. Wiley-VCH, Weinheim.

40. Hashimoto, H., Nishimura, T., Umetsu,Y., (2003). Hydrolysis of Antimony(III)-Hydrochloric Acid Solution at 25°C, Materials Transactions, 44(8), 1624-1629.

41. O'Mara, W.C., Herring, R.B., Hunt, L.P. (1990). Handbook of Semiconductor Silicon Technology. William Andrew. 473.

42. Anderson, C. G. (2012). The metallurgy of antimony. Geochemistry, 72, 3-8.

43. Freedman, L.D., Doak, G.O., Long, G.G., (1992). Antimony compounds. Kirk-Othmer Encyclopedia of Chemical Technology, 3rd ed., Vol.3, John Wiley & Sons Inc., New York.

44. Herbst, K.A., Rose, G., Hanusch, K., Schumann, Wolf, H.U., (1985). Antimony and antimony compounds. Ullmann’s Encyclopedia of Industrial Chemistry, Vol. A3, VCH Publishers.

45. Zirngieble, E. (1986). Metalle in der Umwelt. Chemie Ingenieur Technik, 58(8), 698-698.

46. Marczenko, Z., & Balcerzak, M. (2000). Separation and preconcentration of elements in inorganic analysis. Analytical Spectroscopy Library, 10, 5-25.

47. Tella, M., Pokrovski, G. S. (2009). Antimony(III) complexing with O-bearing organic ligands in aqueous solution: An X-ray absorption fine structure spectroscopy and solubility study. Geochimica et Cosmochimica Acta, 73(2), 268-290.

48. Anderegg, G., & Malik, S. (1970). Die Komplexbildungstendenz des dreiwertigen Antimons in wässeriger Lösung. Helvetica Chimica Acta, 53(3), 577-600.

49. Zheng, J., Iijima, A., & Furuta, N. (2001). Complexation effect of antimony compounds with citric acid and its application to the speciation of antimony(iii) and antimony(v) using HPLC-ICP-MS. Journal of Analytical Atomic Spectrometry, 16(8), 812-818.

50. Filella, M., & May, P. M. (2005). Critical appraisal of available thermodynamic data for the complexation of antimony(iii) and antimony(v) by low molecular mass organic ligands. Journal of Environmental Monitoring, 7(12), 1226.

51. Meier, P. (1978). Temperature dependence of hyperfine fields at impurities in metals. Solid State Communications, 27(11), 1163-1166.

52. Ghosh, J. C., & Kappana, A. N. (1924). Electrodeposition of Antimony. The Journal of Physical Chemistry, 28(2), 149-160.

53. Hu, H., Mo, M., Yang, B., Shao, M., Zhang, S., Li, Q., & Qian, Y. (2003). A rational complexing-reduction route to antimony nanotubes. New Journal of Chemistry, 27(8), 1161.

54. Fouda, A.K. Mohamed, B. (1990). Electrodeposition of Antimony Bulletin of Electrochemistry. 6(7), 677-678.

55. Zhang, Y., Li, G., Wu, Y., Zhang, B., Song, W., & Zhang, L. (2002). Antimony Nanowire Arrays Fabricated by Pulsed Electrodeposition in Anodic Alumina Membranes. Advanced Materials, 14(17), 1227-1230.

56. Bryngelsson, H., Eskhult, J., Edström, K., & Nyholm, L. (2007). Electrodeposition and electrochemical characterisation of thick and thin coatings of Sb and Sb/Sb2O3 particles for Li-ion battery anodes. Electrochimica Acta, 53(3), 1062-1073.

57. Mosby, J. M., & Prieto, A. L. (2008). Direct Electrodeposition of Cu2Sb for Lithium-Ion Battery Anodes. Journal of the American Chemical Society, 130(32), 10656-10661.

58. Eliaz, N., & Gileadi, E. (2008). Induced Codeposition of Alloys of Tungsten, Molybdenum and Rhenium with Transition Metals. Modern Aspects of Electrochemistry, 191-301.

59. Kolbe, F., Mattusch, J., Wennrich, R., Weiss, H., Sorkau, E., Lorenz, W., Daus B., (2012). Analytical investigations of antimony-edta complexes and their use in speciation analysis. Fresenius Environmental Bulletin, 21(11).

60. Liu, L., Hu, Z., Cui, Y., Li, B., & Zhou, X. (2010). A facile route to the fabrication of morphology-controlled Sb2O3 nanostructures. Solid State Sciences, 12(5), 882-886.

61. Han-ying, J., (1984). Physical chemistry of hydrometallurgy. Beijing: Metallurgical Industry Press, 1984.

62. Razeghi, M. (2012). Antimony: Characteristics, Compounds, and Applications. Nova Science Pub., Hauppauge, NY.

63. Xin-ling, D., (2012). Research on the hydrolysis equilibrium of antimony trichloride in the Sb3+-Cl--H2O system. China Nonferrous Metallurgy, 41(5), 75-79.

64. Bratsch, S.G., (1989). Standard Electrode Potentials and Temperature Coefficients in Water at 298.15K. Journal of Physical and Chemical Reference Data, 18(1), 1-21.

65. Van der Pas, V., & Dreisinger, D. (1996). A fundamental study of cobalt cementation by zinc dust in the presence of copper and antimony additives. Hydrometallurgy, 43(1-3), 187-205.

66. Shamsuddin, M. (2016). Physical Chemistry of Metallurgical Processes. Hoboken, NJ: John Wiley & Sons.

67. Lew, R., (1994). The removal of cobalt from zinc sulphate electrolytes using the copper-antimoney process, in Materials Engineering. The University of British Columbia: Vancouver, Canada.

68. Krause, B., Sandenbergh, R. (2015). Optimization of cobalt removal from an aqueous sulfate zinc leach solution for zinc electrowinning. Hydrometallurgy, 155, 132-140.

69. Burger, K., Gaizer, F., & Schulek, E. (1960). Analytical uses of bromine monochlorideDetermination of hydroxylamine. Contributions to the bromic acid-hydrochloric acid reaction. Talanta, 5(2), 97-101.

70. Schulek, E. (1960). Fundamental principles of titrations with potassium bromate. Talanta, 7(1-2), 51-55.

71. Aktas, S. (2008). Silver recovery from silver-rich photographic processing solutions by copper. Canadian Metallurgical Quarterly, 47(1), 37-44.

72. Aktas, S. (2010). Silver recovery from spent silver oxide button cells. Hydrometallurgy, 104(1), 106-111.

73. Boyanov, B. S., Konareva, V. V., & Kolev, N. K. (2004). Purification of zinc sulfate solutions from cobalt and nickel through activated cementation. Hydrometallurgy, 73(1-2), 163-168.

74. Bøckman, O., & Østvold, T. (2000). Products formed during cobalt cementation on zinc in zinc sulfate electrolytes. Hydrometallurgy, 54(2-3), 65-78.

CURRICULUM VITAE

Name, Surname: Abdullah UYSAL

Birthplace and Date: İzmit, 04/08/1986

Email: a.uysal@ymail.com

Education

Country	University	Faculty / Institute	Program	Derece	Graduation Year
TR	Kocaeli University	Mühendislik	Metallurgical and Materials Engineering	2.31	2013
TR	Marmara University	Fen Bilimleri	Metallurgical and Materials Engineering	3.86	-

Work Experiences

Period	Company / Institution	Job
2016 - 2017	Gürmetal Hassas Döküm Ltd.Şti	Project Engineer
2015 - 2016	Arpek Arkan Alüminyum Enjeksiyon Kalıp A.Ş	Proses Quality Engineer
2014 - 2015	IHI Infrastructure Systems Co.Ltd (İzmit Körfez Geçiş Köprü Projesi)	Production Quality Engineer
2011 - 2013	Ertuğ Metal Döküm ve Makina Ltd.Şti.	Production Quality Engineer